

Transverse Spin Supercurrent at p -wave magnetic Josephson Junctions

Morteza Salehi¹

¹*Physics Department, Bu-Ali Sina University, Hamadan, Iran**

(Dated: July 16, 2025)

We theoretically study a Josephson junction consisting of s -wave superconductors and a p -wave magnet. We find that in the presence of a strength vector of p -wave magnet, the electrons' and holes' dispersion relation shifts in the k -space. Additionally, we demonstrate that the perpendicular component of the strength vector converts Andreev bound states into Andreev modes that can propagate along the junction's interfaces. These modes create a transverse spin supercurrent while their transverse charge supercurrent is zero. These features open an opportunity to design superconducting spintronics devices.

Introduction - The interplay between magnetism and superconductivity has led to the discovery of remarkable phenomena including spin-triplet superconductivity, topological superconducting states, and non-reciprocal charge transport [1–5]. Recent advances in unconventional magnet (uM) has revealed new possibilities through materials like d -wave altermagnet (dAM) and p -wave magnet (pM) that combine zero net magnetization with non-relativistic spin splitting [6–14].

The uMs are characterized by zero net magnetization and their parity-dependent spin splitting: d -wave types preserve inversion symmetry while breaking time-reversal symmetry, whereas p -wave types maintain time-reversal symmetry but break inversion symmetry [14, 15]. Although magnets can be used to produce spin current, their magnetization bring challenges for spin transport [16]. In contrast, the uMs are promising candidates for generating spin currents [17]. In superconducting junctions, the $dAMs$ [18, 19] have been shown to induce $0-\pi$ transitions [20–24], diode effect [25–27], oriented-dependent Andreev reflection [28–30], crossed Andreev reflection [31, 32], and generate odd-frequency pairing [33]. Also, the interplay of pMs and superconductors are attracting attentions [34–39].

In this Letter, we theoretically study a Josephson junction formed by s -wave superconductors and a pM . The pM strength vector splits spin-dependent bands, and its transverse component generates propagating Andreev modes along the junction interfaces. These modes carry a transverse spin supercurrent without a charge counterpart, offering a platform for dissipationless spin transport in superconducting spintronics [40].

Model and formalism— As shown in Fig. 1(a), our 2D model consists of a pM between two semi-infinite s -wave superconductors. We employ the Bogoliubov-de Gennes (BdG) formalism to obtain the Andreev bound states and their related charge and spin supercurrents [41]. In the absence of spin-mixing potential, the s -wave superconducting pair potential, Δ_0 , couples the spin- \uparrow electrons with spin- \downarrow holes and vice versa. So, the BdG Hamiltonian is [35–37, 41, 42],

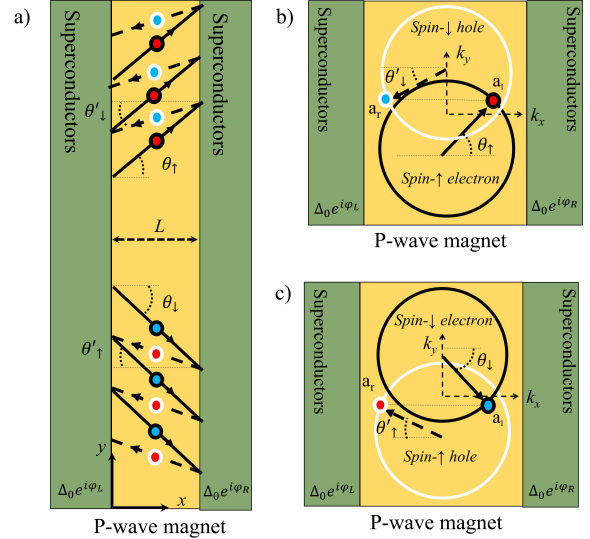


FIG. 1. (a) The p -wave magnet Josephson junction in real space. The black solid arrows show the propagation direction of electron particles, where the black dashed arrows demonstrate the reflected hole particles in the pM region. The black circles with red (blue) dots demonstrate the electron-like quasi particles with spin- \uparrow (\downarrow) configuration. The white circles with red (blue) dots illustrate hole particles with spin- \uparrow (\downarrow) configuration. The α_y creates the Andreev modes that propagate parallel to the interface of the junction. (b) The spin- \uparrow electrons' and spin- \downarrow holes' Fermi circles in the k -space that shift related to each other in the presence of $\alpha \neq 0$. These Andreev modes produce a positive spin supercurrent in the y -direction of real space. Here, we set $(\alpha_x = 0, \alpha_y \neq 0)$. (c) The spin- \downarrow electrons' and spin- \uparrow holes' Fermi circles that produce negative spin supercurrent in the $-y$ -direction of real space.

$$\mathcal{H}_{\pm}(\mathbf{k}) = \begin{pmatrix} \frac{\hbar^2}{2m}(\mathbf{k} \pm \boldsymbol{\alpha})^2 - \mu & \Delta_0 e^{i\phi} \\ \Delta_0 e^{-i\phi} & \mu - \frac{\hbar^2}{2m}(\mathbf{k} \mp \boldsymbol{\alpha})^2 \end{pmatrix}. \quad (1)$$

The $\mathcal{H}_+(\mathbf{k})$ acts on basis $\Psi = (\psi_{\uparrow}, -\psi_{\downarrow}^*)$ while the $\mathcal{H}_-(\mathbf{k})$ works with $\Psi = (\psi_{\downarrow}, \psi_{\uparrow}^*)$. Also, the 2D wave vector, $\mathbf{k} = (k_x, k_y)$, hosts the $\boldsymbol{\alpha}$ as pM strength vector. The μ is a Fermi energy that can be different in S and pM regions. Since ϕ stands for superconductivity phase, we

define $\delta\phi = \phi_R - \phi_L$ as superconducting phase difference between right and left superconductors that produces supercurrents[43]. We take the junction in x -direction where pM region, ($\alpha \neq 0, \Delta_0 = 0$), is located at $0 \leq x \leq L$. The eigenvalues of $\mathcal{H}_+(\mathbf{k})$ for spin- \uparrow electron excitations in the pM region are,

$$\epsilon_e = (\hbar^2 ((k_x + \alpha_x)^2 + (k_y + \alpha_y)^2) / 2m) - \mu. \quad (2)$$

. This dispersion relation shows a parabola in the k -space. For a fixed energy, the states of spin- \uparrow electrons form a Fermi circle with the radius of $q_e = \sqrt{2m(\epsilon_e + \mu)/\hbar^2}$, centered at $(-\alpha_x, -\alpha_y)$, as depicted schematically in Fig.1 (b). The propagation direction of each state in real space can be obtained via $\mathbf{V}_e = \partial\epsilon_e/\hbar\partial\mathbf{k}$. The state a_I located on the spin- \uparrow electron's Fermi circle moves with the angle of θ_\uparrow with respect to the x -direction in real space. The spin- \downarrow holes of $\mathcal{H}_+(\mathbf{k})$ have energy dispersion of $\epsilon_h = (-\hbar^2 ((k'_x - \alpha_x)^2 + (k'_y - \alpha_y)^2) / 2m) + \mu$. This relation gives rise to another Fermi circle with radius $q_h = \sqrt{2m|\epsilon - \mu|/\hbar^2}$, centered at (α_x, α_y) for a fixed energy value. In the same scenario, their propagation angle, θ'_\downarrow , are determined by the group velocity, $\mathbf{V}_h = -\partial\epsilon_h/\hbar\partial\mathbf{k}$.

The spin- \uparrow hitting electron to the superconductor interface from the non-superconducting side of the Josephson junction can be reflected as a spin- \downarrow hole during the Andreev process to transfer an s-wave Cooper pair into the superconducting lead[44]. The reflected hole can be back-scattered again as an electron from the other surface of the Josephson junction and creates an Andreev-bound state in non-superconducting region [45, 46]. In the ballistic limit, the energy and parallel component of the wave vector with respect to the junction's interface, k_y , are conserved during the scattering processes. In the presence of $\alpha_y \neq 0$, where the electrons' and holes' Fermi circles shift in k_y -direction oppositely, the Andreev process occurs just in the overlap zone of two Fermi circles[47]. As shown in Fig.1(a), the Andreev bound states convert to Andreev modes and propagate parallel to the junction's interfaces. [48, 49]. The contribution of each Andreev mode to the transverse charge supercurrent is proportional to $\sim (\partial\epsilon_+/\partial\delta\phi)(\sin\theta_\uparrow + \mathcal{S}\sin\theta'_\downarrow)$. Also, its share to the transverse spin supercurrent is $\sim (\partial\epsilon_+/\partial\delta\phi)(\sin\theta_\uparrow - \mathcal{S}\sin\theta'_\downarrow)$. Here, $\mathcal{S} = \text{sign}(\mu - \epsilon)$ determines the location of the reflected hole in conduction or valence band[50]. Also, $\epsilon_+(\delta\phi)$ is the energy-phase relation (EPR) of Andreev modes.

On the other hand, $\mathcal{H}_-(\mathbf{k})$ has a similar scenario with spin- \downarrow electron and its related spin- \uparrow hole. In contrast to spin- \uparrow electrons, the dispersion relation of spin- \downarrow electrons is centered at (α_x, α_y) . As depicted in Fig.1(c), the origin of the spin- \uparrow holes' dispersion relation is at $(-\alpha_x, -\alpha_y)$. Due to this reverse adjustment of spin-dependent dispersion relation in k -space, the Andreev modes with EPR of $\epsilon_-(\delta\phi)$, propagate opposite

to the Andreev modes with EPR of $\epsilon_+(\delta\phi)$. The transverse charge supercurrent of $\epsilon_-(\delta\phi)$ cancels the share of $\epsilon_+(\delta\phi)$, whereas the resulting transverse spin supercurrent of $\epsilon_-(\delta\phi)$ sums up the share of $\epsilon_+(\delta\phi)$ with a factor of 2. As shown in Fig.1(a), a pure transverse spin supercurrent flows parallel to the junction interfaces, whereas there is no transverse charge supercurrent.

The overlap of two Fermi circles determines the critical angles of θ_\uparrow , where within those values the Andreev modes are real and stable. Since the parallel component of the wave vector, $k'_y = k_y$, and the energy of excitations, $\epsilon_e = \epsilon_h = \epsilon$ are conserved during the Andreev process, we use the x -component of the hole wave vector to obtain the critical angles in the $\alpha_y \neq 0$ case,

$$k'_x = \pm \sqrt{\frac{2m}{\hbar^2}(\mu - \epsilon) - (k_y - \alpha_y)^2}. \quad (3)$$

The k'_x must be real to have stable Andreev modes. From $k_y = q_e \sin\theta_\uparrow - \alpha_y$, the lower and upper critical angles of Andreev modes for $\mathcal{H}_+(\mathbf{k})$ can be obtained. In a similar way for $\mathcal{H}_-(\mathbf{k})$ we have,

$$\begin{aligned} \theta_{min}^\pm &= \sin^{-1} \left(\max \left\{ -1, \frac{-q_h \pm 2\alpha_y}{q_e} \right\} \right) \\ \theta_{max}^\pm &= \sin^{-1} \left(\min \left\{ 1, \frac{q_h \pm 2\alpha_y}{q_e} \right\} \right). \end{aligned} \quad (4)$$

To obtain $\epsilon_+(\delta\phi)$ from $\mathcal{H}_+(\mathbf{k})$, we begin with the right and left mover wave functions of spin- \uparrow electrons in pM region,

$$\psi_{e,\uparrow}^\pm(\mathbf{r}) = \frac{1}{\sqrt{V_{e,x}}} \begin{pmatrix} 1 \\ 0 \end{pmatrix} e^{\pm i q_e \cos\theta_\uparrow x - i \alpha_x x} e^{i k_y y}. \quad (5)$$

Here, $V_{e,x}$ is the x -component of the group velocity and acts as a normalization factor of probability conservation. The \pm sign refers to the propagation direction with respect to x -axis in real space. Also, the spin- \downarrow hole wave functions are,

$$\psi_{h,\downarrow}^\pm(\mathbf{r}) = \frac{1}{\sqrt{V_{h,x}}} \begin{pmatrix} 0 \\ 1 \end{pmatrix} e^{\mp i q_h \cos\theta'_\downarrow x + i \alpha_x x} e^{i k_y y}. \quad (6)$$

Due to the different scattering processes, the whole wave function in the pM region is[51],

$$\Psi_{pM}(\mathbf{r}) = a_1 \psi_{e,\uparrow}^+(\mathbf{r}) + a_2 \psi_{e,\uparrow}^-(\mathbf{r}) + a_3 \psi_{h,\downarrow}^+(\mathbf{r}) + a_4 \psi_{h,\downarrow}^-(\mathbf{r}). \quad (7)$$

One can calculate the electron-like and hole-like excitations of the superconducting region, ($\alpha = 0, \Delta_0 \neq 0$), as below,

$$\begin{aligned} \psi_e^{S,\pm}(\mathbf{r}) &= \frac{1}{\sqrt{V_s}} \begin{pmatrix} e^{i\beta} \\ e^{-i\phi} \end{pmatrix} e^{\pm i k_{e,x}^S x} e^{i k_y y} \\ \psi_h^{S,\pm}(\mathbf{r}) &= \frac{1}{\sqrt{V_s}} \begin{pmatrix} e^{i\phi} \\ e^{i\beta} \end{pmatrix} e^{\mp i k_{h,x}^S x} e^{i k_y y}. \end{aligned} \quad (8)$$

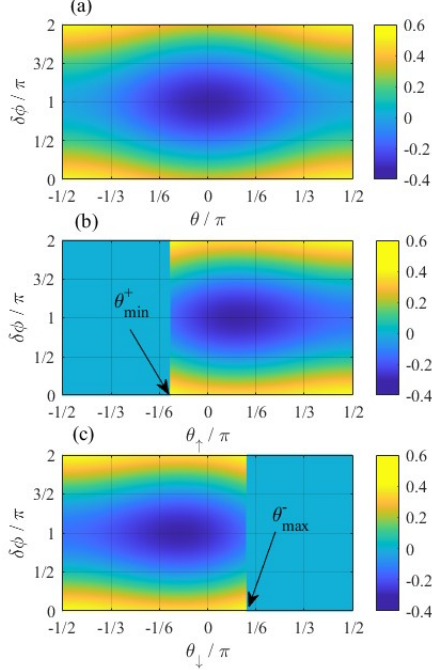


FIG. 2. (a) The EPR of the Josephson junction in the absence of pM strength vector. In this case, the $\varepsilon_+(\delta\phi)$ and $\varepsilon_-(\delta\phi)$ are degenerate. Here, we set $\mu = \Delta_0$, $\mu_S = 10\Delta_0$ and $L = \kappa_0^{-1}$. (b) The $\varepsilon_+(\delta\phi)$ with respect to the propagation direction of spin- \uparrow incoming electron. The EPR becomes imaginary for $\theta_+ < \theta_{min}^+$. (c) The $\varepsilon_-(\delta\phi)$ with respect to the propagation angle of spin- \downarrow incoming electrons. Here, $\varepsilon_-(\delta\phi)$ becomes evanescent for $\theta_{max}^- < \theta_+$. Also, we set $\alpha_y = 0.3\kappa_0$.

We define $\beta = \cos^{-1}(\epsilon/\Delta_0)$. Also, $k_{e(h),x}^S$ and V_S are the x -component of electron (hole) wave vector and group velocity in the superconductor region, respectively. In a similar way, we write the whole wave functions of right and left superconductor,

$$\begin{aligned}\Psi_L^S(\mathbf{r}) &= a_5\psi_e^{S,-}(\mathbf{r}) + a_6\psi_h^{S,-}(\mathbf{r}) \\ \Psi_R^S(\mathbf{r}) &= a_7\psi_e^{S,+}(\mathbf{r}) + a_8\psi_h^{S,+}(\mathbf{r}).\end{aligned}\quad (9)$$

Here, a_j with $j = \{1, \dots, 8\}$ is the related probability amplitude of each moving wave function. The first boundary condition confirms the continuity of wave functions at interfaces,

$$\begin{aligned}\Psi_L^S(x=0) &= \Psi_{pM}(x=0) \\ \Psi_{pM}(x=L) &= \Psi_R^S(x=L),\end{aligned}\quad (10)$$

while the second boundary condition satisfies the conservation of probability distribution[36, 52, 53],

$$\begin{aligned}V^S\Psi_L^S(x=0) &= V_{e(h),x}\Psi_{pM}(x=0) \\ V_{e(h),x}\Psi_{pM}(x=L) &= V^S\Psi_R^S(x=0).\end{aligned}\quad (11)$$

EPR– The energy-phase relation of the Josephson junction can be obtained via the Eqs (10) and (11). They

lead to eight homogeneous equations for probability amplitudes of a_j . To have nontrivial solutions, the determinant of its coefficient matrix must be zero. We focus on the short-junction regime ($\epsilon \ll \mu$) to have experimentally possible results. The transverse spin supercurrent emerges in the presence of $\alpha_y \neq 0$. With these assumptions, the EPR of $\mathcal{H}_+(\mathbf{k})$ can be calculated with the simplification of the determinant such as

$$\varepsilon_+(\delta\phi) = \Delta_0 \cos \left(\frac{1}{2} \cos^{-1} \left(\frac{\mathcal{A} \cos \delta\phi - \mathcal{D}}{\sqrt{\mathcal{B}^2 + \mathcal{C}^2}} \right) + \frac{1}{2} \cos^{-1} \left(\frac{\mathcal{B}}{\sqrt{\mathcal{B}^2 + \mathcal{C}^2}} \right) \right). \quad (12)$$

where we use,

$$\mathcal{A} = 4q^2 \cos \theta_+ \cos \theta'_\downarrow,$$

$$\begin{aligned}\mathcal{B} &= 4q^2 \cos(k_x L) \cos(k'_x L) \cos \theta_+ \cos \theta'_\downarrow \\ &\quad + (1 + q^2 \cos^2 \theta_+)(1 + q^2 \cos^2 \theta'_\downarrow) \sin(k_x L) \sin(k'_x L),\end{aligned}$$

$$\begin{aligned}\mathcal{C} &= 2q(1 + q^2 \cos^2 \theta_+) \cos \theta'_\downarrow \sin(k_x L) \cos(k'_x L) \\ &\quad + 2q(1 + q^2 \cos^2 \theta'_\downarrow) \cos \theta_+ \cos(k_x L) \sin(k'_x L),\end{aligned}$$

$$\mathcal{D} = -(1 - q^2 \cos^2 \theta_+)(1 - q^2 \cos^2 \theta'_\downarrow) \sin(k_x L) \sin(k'_x L). \quad (13)$$

Here, $q = \sqrt{\mu/\mu_s}$ is the square root of the relative Fermi energies. Also, k_x can be obtained from Eq.(2). As shown in part (a) of Fig.(1), the $\varepsilon_+(\delta\phi)$ and $\varepsilon_-(\delta\phi)$ are degenerate in the absence of the pM strength vector. Since α_x does not contribute to the transverse spin supercurrent, we set $\alpha_x = 0$. We normalize all energy scales with the superconducting gap, Δ_0 . Moreover, the superconducting wave vector, $\kappa_0 = (2m\Delta_0/\hbar^2)^{1/2}$, is used to normalize the wave vectors. In the presence of $\alpha_y \neq 0$, the electrons' and holes' Fermi circles shift oppositely in the k_y -direction and overlap partially. The Andreev modes are created in this overlap zone, and their propagation directions are confined between the thresholds defined by Eq.(4). In part (b) and (c) of Fig.(2), the EPRs of $\mathcal{H}_+(\mathbf{k})$ and $\mathcal{H}_-(\mathbf{k})$ are depicted. For spin- \uparrow electrons with propagation direction beyond the critical values of Eq.(4), the $\varepsilon_+(\delta\phi)$ becomes evanescent and cannot participate in the transverse charge and spin supercurrents. Similarly, $\varepsilon_-(\delta\phi)$ cannot propagate in $\theta_{max}^- < \theta_+$.

Charge Supercurrent– The charge supercurrent at zero temperature that passes through the junction interfaces is given by [48, 49, 54]

$$\frac{I_J(\delta\phi)}{I_0} = \sum_{\gamma=\pm} \int_{-\pi/2}^{\pi/2} \frac{-\partial \varepsilon_\gamma(\delta\phi)}{\partial \delta\phi} (\cos \theta_{\uparrow(\downarrow)} + \cos \theta'_{\downarrow(\uparrow)}) d\theta_{\uparrow(\downarrow)}. \quad (14)$$

Here, $I_0 = 2e\Delta_0\mathcal{N}(\mu)/\hbar$ is the normalized ballistic supercurrent, where $\mathcal{N}(\mu)$ is the density of states at the Fermi energy. The Andreev modes of $\varepsilon_\gamma(\delta\phi)$ have two parts: incoming electrons with propagation direction of $\theta_{\uparrow(\downarrow)}$ and

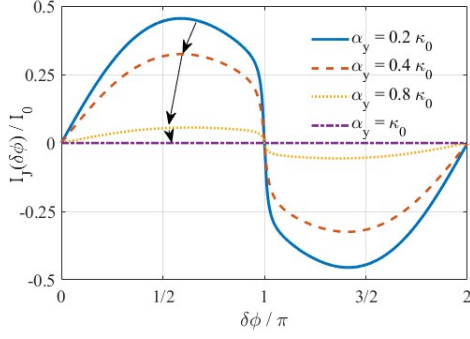


FIG. 3. The charge supercurrent that passes through the Josephson junction vs superconducting phase difference. An increase in α_y decreases the charge supercurrent. Further increase, $\kappa_0 \leq \alpha_y$, does not lead to $0 - \pi$ transition. The other inputs are same as Fig.(2.)

reflecting holes with propagation direction of $\theta'_{\downarrow(\uparrow)}$. The $\cos \theta_{\uparrow(\downarrow)}$ determines the share of the first one with respect to the x -direction, whereas the $\cos \theta'_{\downarrow(\uparrow)}$ takes the share of last part into account. In the short-junction regime, the Andreev modes have a dominant role in the Josephson current. For incoming electrons with propagation direction beyond the critical angles of Eq.(4), there is a negligible chance of co-tunneling for Cooper pairs to pass the Josephson junction that we ignore in our calculations[48, 55]. The charge supercurrent that flows in the junction is depicted in Fig.(3) for different values of α_y . An increase in α_y reduces the overlapping region between the electron and hole Fermi circles, as depicted in Fig.(1). This also reduces the charge supercurrent that flows in the junction. For $k_F \leq \alpha_y$, where $k_F = (2m\mu/\hbar^2)^{1/2}$, the overlap zone disappears and the charge supercurrent tends to zero. More increase in α_y cannot change the sign of charge supercurrent and we do not encounter the π -junction[56]. The transverse charge supercurrent can be calculated via,

$$\frac{I_J^t(\delta\phi)}{I_0} = \sum_{\gamma=\pm} \int_{\theta_{min}^{\gamma}}^{\theta_{max}^{\gamma}} \frac{-\partial \varepsilon_{\gamma}(\delta\phi)}{\partial \delta\phi} (\sin \theta_{\uparrow(\downarrow)} + \mathcal{S} \sin \theta'_{\downarrow(\uparrow)}) d\theta_{\uparrow(\downarrow)}. \quad (15)$$

Here, the contribution of electron and hole parts of Andreev modes with respect to the y -direction is calculated by $\sin \theta_{\uparrow(\downarrow)}$ and $\sin \theta'_{\downarrow(\uparrow)}$, respectively. As its obvious from Fig.(1) and can be calculated from Eq.(15), the transverse charge supercurrent of $\varepsilon_+(\delta\phi)$ cancel out with the contribution of $\varepsilon_-(\delta\phi)$. It means there is no transverse charge supercurrent flowing in the pM region of the Josephson junction.

Spin Supercurrent— The electronic part of each Andreev mode carry the amount of $(-\partial \varepsilon_{\gamma}/\partial \delta\phi) \gamma \hbar \cos \theta_{\uparrow(\downarrow)}/2$ spin supercurrent in x -direction whereas this quantity for hole part is

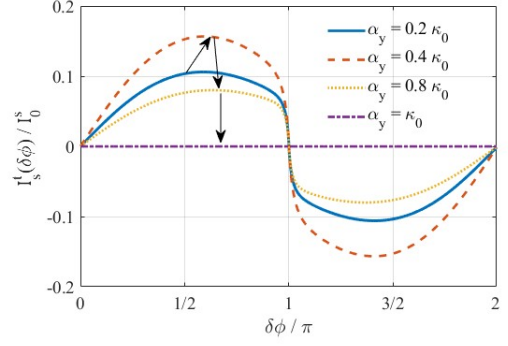


FIG. 4. The transverse spin supercurrent that flows parallel to the Josephson junction's interfaces. Appearance of α_y creates a transverse spin supercurrent. The normalized spin supercurrent is $I_0^s = \hbar I_0/2$. The other inputs are same as Fig.(2.)

$(-\partial \varepsilon_{\gamma}/\partial \delta\phi) \gamma \hbar \cos \theta'_{\downarrow(\uparrow)}/2$. So, the spin supercurrent in the x -direction can be calculated via,

$$\frac{I_s(\delta\phi)}{I_0^s} = \sum_{\gamma=\pm} \int_{-\pi/2}^{\pi/2} \gamma \frac{-\partial \varepsilon_{\gamma}(\delta\phi)}{\partial \delta\phi} (\cos \theta_{\uparrow(\downarrow)} - \cos \theta_{\downarrow(\uparrow)}) d\theta_{\uparrow(\downarrow)}. \quad (16)$$

Here, the normalized ballistic spin supercurrent is $I_0^s = \hbar I_0/2e$. Due to the s-wave character of two superconducting leads, there is no spin supercurrent to flow in the x -direction of the junction.

On the other hand, the contribution of $\varepsilon_+(\delta\phi)$ to spin supercurrent in y -direction is given by, $\hbar(-\partial \varepsilon_+/\partial \delta\phi)(\sin \theta_{\uparrow} - \mathcal{S} \sin \theta'_{\downarrow})/2$ while the contribution that comes from $\varepsilon_-(\delta\phi)$ is equal $\hbar(-\partial \varepsilon_-/\partial \delta\phi)(\sin \theta_{\downarrow} - \mathcal{S} \sin \theta'_{\uparrow})/2$. So, the transverse spin supercurrent in y -direction is given by,

$$\frac{I_s^t(\delta\phi)}{I_0^s} = \sum_{\gamma=\pm} \int_{\theta_{min}^{\gamma}}^{\theta_{max}^{\gamma}} \gamma \frac{-\partial \varepsilon_{\gamma}(\delta\phi)}{\partial \delta\phi} (\sin \theta_{\uparrow(\downarrow)} - \mathcal{S} \sin \theta_{\downarrow(\uparrow)}) d\theta_{\uparrow(\downarrow)}. \quad (17)$$

In the presence of $0 \leq \alpha_y$, only the Andreev modes of $\varepsilon_+(\delta\phi)$ survive in the range of $\theta_{min}^- \leq \theta_{\uparrow} \leq \theta_{max}^+$ while the Andreev modes of $\varepsilon_-(\delta\phi)$ is evanescent. This creates a positive spin supercurrent in y -direction. A reverse situation occurs in the range of $\theta_{min}^+ \leq \theta_{\downarrow} \leq \theta_{max}^-$ where the Andreev modes of $\varepsilon_+(\delta\phi)$ become evanescent while their $\varepsilon_-(\delta\phi)$ counterparts are propagating. This leads to a negative spin supercurrent in $-y$ -direction. So, the summation of these two terms with the zero value of Eq.(15) for transverse charge supercurrent leads to a purely transverse spin supercurrent that flows in the pM region parallel with Josephson's interfaces. We illustrate the transverse spin supercurrent for different values of α_y in Fig.(4). As α_y increases from zero, the transverse

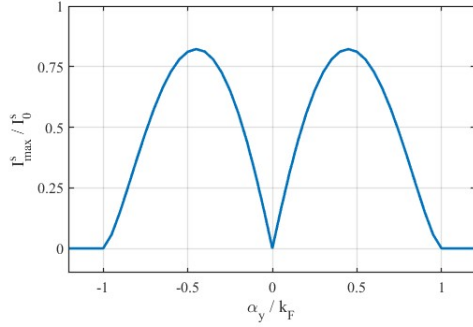


FIG. 5. The critical values of transverse spin supercurrent vs α_y .

spin supercurrent in the junction begins to flow. With a further increase in α_y , the spin supercurrent increases and reaches its maximum. As shown in Fig.(5), beyond this point, $\alpha_y \sim k_F/2$, further increase in α_y leads to a decrease in the spin supercurrent.

Now, we aim to predict the results that can be obtained in experiments. The typical length of a ballistic Josephson junction is $L \sim 1 \mu\text{m}$, and we assume the width to be $W \sim 1 \mu\text{m}$. The typical value of the superconducting gap is $\Delta_0 \sim 1 \text{ meV}$, and the Fermi energy is assumed to be comparable to the superconducting gap. This leads to a Fermi wave vector of approximately $k_F \sim 1.33 \times 10^8 \text{ m}^{-1}$. Accordingly, the available density of modes in the junction is estimated as $\mathcal{N}(\mu) = k_F W / \pi \sim 50$. This implies that the ballistic charge supercurrent is approximately $I_0 \sim 100 \mu\text{A}$. Based on Fig.(3), the predicted charge supercurrent flowing through the $p\text{M}$ Josephson junction is in the range $I_J \sim 10\text{--}50 \mu\text{A}$. Finally, the estimated transverse spin supercurrent flowing parallel to the Josephson interfaces is $I_s^t \sim 3.1 \times 10^6 \hbar/\text{s}$, which is fully detectable using currently available instruments.

Conclusion– To summarize, we have studied the unconventional p -wave magnetic Josephson junction. It is found that electrons' and holes' dispersion relations shift in k -space in the presence of p -wave magnet strength vector. The perpendicular component of α converts the Andreev bound states into Andreev modes that can propagate alongside the Junction's interfaces. We show that these modes create a transverse spin supercurrent while the transverse charge supercurrent is zero. We believe this prediction can be detected with available technology and can be used to design future superconducting spintronics devices.

Acknowledgment– M. S. thanks R. Beiranvand for fruitful discussion.

* m.salehi@basu.ac.ir

- [1] A. I. Buzdin, Proximity effects in superconductor-ferromagnet heterostructures, *Rev. Mod. Phys.* **77**, 935 (2005)
- [2] I. Mazin and D. J. Singh, Ferromagnetic spin fluctuation induced superconductivity in Sr 2 RuO 4 , *Phys. Rev. Lett.* **79**, 733 (1997).
- [3] F. S. Bergeret, A. F. Volkov, and K. B. Efetov, Odd triplet superconductivity and related phenomena in superconductor-ferromagnet structures, *Rev. Mod. Phys.* **77**, 1321 (2005).
- [4] A. F. Volkov, F. S. Bergeret, and K. B. Efetov, Odd Triplet Superconductivity in Superconductor-Ferromagnet Multilayered Structures, *Phys. Rev. Lett.* **90**, 117006 (2003).
- [5] M. Sato and Y. Ando, *Rep. Prog. Phys.* **80**, 076501 (2017).
- [6] Libor Šmejkal, Rafael González-Hernández, T. Jungwirth, and J. Sinova, Crystal time-reversal symmetry breaking and spontaneous Hall effect in collinear antiferromagnets, *Sci. Adv.* **6**, eaaz8809.
- [7] Igor Mazin and P. R. X. Editors The, Editorial: Altermagnetism—A New Punch Line of Fundamental Magnetism, *Phys Rev X* **12**, 040002 (2022).
- [8] Tomas Jungwirth, Rafael M Fernandes, Jairo Sinova, and Libor Šmejkal, Altermagnets and beyond: Nodal magnetically-ordered phases, [arXiv:2409.10034](https://arxiv.org/abs/2409.10034) (2024).
- [9] T Jungwirth, RM Fernandes, E Fradkin, AH MacDonald, J Sinova, and L Šmejkal, Altermagnetism: an unconventional spin-ordered phase of matter, [arXiv:2411.00717](https://arxiv.org/abs/2411.00717) (2024).
- [10] Libor Šmejkal, Jairo Sinova, and Tomas Jungwirth, Emerging Research Landscape of Altermagnetism, *Phys Rev X* **12**, 040501 (2022).
- [11] Libor Šmejkal, Jairo Sinova, and Tomas Jungwirth, Beyond Conventional Ferromagnetism and Antiferromagnetism: A Phase with Nonrelativistic Spin and Crystal Rotation Symmetry, *Phys. Rev. X* **12**, 031042 (2022).
- [12] Qian Song, Srdjan Stavić, Paolo Barone, Andrea Droghetti, Daniil S. Antonenko, Jörn W. F. Venderbos, Connor A. Occhialini, Batyr Ilyas, Emre Ergeçen, Nuh Gedik, Sang-Wook Cheong, Rafael M. Fernandes, Silvia Picozzi, and Riccardo Comin, Electrical switching of a p -wave magnet, *Nature* **642**, 64 (2025).
- [13] Bjørnulf Brekke, Pavlo Sukhachov, Hans Glöckner Güll, Arne Brataas, and Jacob Linder, Minimal Models and Transport Properties of Unconventional p -Wave Magnets, *Phys. Rev. Lett.* **133**, 236703 (2024).
- [14] Anna Birk Hellenes, Tomáš Jungwirth, Rodrigo Jaeschke-Ubiergo, Atasi Chakraborty, Jairo Sinova, and Libor Šmejkal, P -wave magnets, [arXiv 2309.01607v01603](https://arxiv.org/abs/2309.01607) (2023).
- [15] Javier Sivianes, Flaviano José dos Santos, and Julen Ibañez-Azpiroz, Optical Signatures of Spin Symmetries in Unconventional Magnets, *Phys. Rev. Lett.* **134**, 196907 (2025).
- [16] I. Žutić, J. Fabian, and S. Das Sarma, Spintronics: Fundamentals and applications, *Rev. Mod. Phys.* **76**, 323 (2004).
- [17] H. Chen, Z. Wang, P. Qin, Z. Meng, X. Zhou, X. Wang, L. Liu, G. Zhao, Z. Duan, T. Zhang, J. Liu, D. Shao, C.

- Jiang, and Z. Liu, Spin-Splitting Magnetoresistance in Altermagnetic RuO₂ Thin Films, *Adv. Mater.*, **2507764**.
- [18] B. Brekke, A. Brataas, and A. Sudbø, Two-dimensional altermagnets: Superconductivity in a minimal microscopic model, *Phys. Rev. B* **108**, 224421 (2023).
- [19] Song-Bo Zhang, Lun-Hui Hu, and Titus Neupert, Finite-momentum Cooper pairing in proximitized altermagnets, *Nat. Commun.* **15**, 1801 (2024).
- [20] B. Lu, K. Maeda, H. Ito, K. Yada, and Y. Tanaka, ϕ -Josephson Junction Induced by Altermagnetism, *Phys. Rev. Lett.* **133**, 226002 (2024).
- [21] Jabir Ali Ouassou, Arne Brataas, and Jacob Linder, dc Josephson Effect in Altermagnets, *Phys. Rev. Lett.* **131**, 076003 (2023).
- [22] C. W. J. Beenakker and T. Vakhtel, Phase-shifted Andreev levels in an altermagnet Josephson junction, *Phys. Rev. B* **108**, 075425 (2023).
- [23] H. P. Sun, S. B. Zhang, C. A. Li, and B. Trauzettel, Tunable second harmonic in altermagnetic Josephson junctions, *Phys. Rev. B* **111**, 165406 (2025).
- [24] Q. Cheng and Q. F. Sun, Orientation-dependent Josephson effect in spin-singlet superconductor/altermagnet/spin-triplet superconductor junctions, *Phys. Rev. B* **109**, 024517 (2024).
- [25] G. Sim and J. Knolle, Pair density waves and supercurrent diode effect in altermagnets, [arXiv:2407.01513](https://arxiv.org/abs/2407.01513) (2024).
- [26] S. Banerjee and M. S. Scheurer, Altermagnetic superconducting diode effect, *Phys. Rev. B* **110**, 024503 (2024).
- [27] Q. Cheng, Y. Mao, and Q. F. Sun, Field-free Josephson diode effect in altermagnet/normal metal/altermagnet junctions, *Phys. Rev. B* **110**, 014518 (2024).
- [28] Chi Sun, Arne Brataas, and Jacob Linder, Andreev reflection in altermagnets, *Phys. Rev. B* **108**, 054511 (2023).
- [29] Michał Papaj, Andreev reflection at the altermagnet-superconductor interface, *Phys. Rev. B* **108**, L060508 (2023).
- [30] Yutaro Nagae, Andreas P. Schnyder, and Satoshi Ikegaya, Spin-polarized specular Andreev reflections in altermagnets, *Phys. Rev. B* **111**, L100507 (2025).
- [31] Sachchidanand Das and Abhiram Soori, Crossed Andreev reflection in altermagnets, *Phys. Rev. B* **109**, 245424 (2024).
- [32] Zhi Ping Niu and Yong Mei Zhang, Electrically controlled crossed Andreev reflection in altermagnet/superconductor/altermagnet junctions, *Supercond. Sci. Technol.* **37**, 055012 (2024).
- [33] D. Chakraborty and A. M. Black-Schaffer, Constraints on superconducting pairing in altermagnets, [arXiv:2408.03999](https://arxiv.org/abs/2408.03999) (2024).
- [34] Y. Fukaya, K. Maeda, K. Yada, J. Cayao, Y. Tanaka, and B. Lu, Josephson effect and odd-frequency pairing in superconducting junctions with unconventional magnets, *Phys. Rev. B* **111**, 064502 (2025).
- [35] K. Maeda, Y. Fukaya, K. Yada, B. Lu, Y. Tanaka, and J. Cayao, Classification of pair symmetries in superconductors with unconventional magnetism, *Phys. Rev. B* **111**, 144508 (2025).
- [36] K. Maeda, B. Lu, K. Yada, and Y. Tanaka, Theory of Tunneling Spectroscopy in Unconventional p-Wave Magnet-Superconductor Hybrid Structures, *J. Phys. Soc. Jpn* **93**, 114703 (2024).
- [37] Y. Nagae, L. Katayama, and S. Ikegaya, Majorana flat bands and anomalous proximity effects in p-wave magnet-superconductor hybrid systems, [arXiv:2502.02053](https://arxiv.org/abs/2502.02053) (2025).
- [38] S. Hong, M. J. Park, and K. Kim, Unconventional p-wave and finite-momentum superconductivity induced by altermagnetism through the formation of Bogoliubov Fermi surface, *Phys. Rev. B* **111**, 054501 (2025).
- [39] Z. Sun, X. Feng, Y. Xie, B. T. Zhou, J. Hu, and K. T. Law, Pseudo-Ising superconductivity induced by p-wave magnetism, [arXiv:2501.10960](https://arxiv.org/abs/2501.10960) (2025).
- [40] J. Linder and J. W. A. Robinson, Superconducting spintronics, *Nat Phys* **11**, 307 (2015).
- [41] P. G. deGennes, Superconductivity of Metals and Alloys, (CRC Press, 1999).
- [42] Pavlo Sukhachov, Hans Glöckner Gilil, Bjørnulf Brekke, and Jacob Linder, Coexistence of p-wave magnetism and superconductivity, *Phys. Rev. B* **111**, L220403 (2025).
- [43] B. D. Josephson, Possible new effects in superconductive tunnelling, *Phys Lett* **1**, 251 (1962).
- [44] AF Andreev, Thermal conductivity of the intermediate state of superconductors, *Sov. Phys. JETP* **20**, 1490 (1965).
- [45] PG De Gennes and Daniel Saint-James, Elementary excitations in the vicinity of a normal metal-superconducting metal contact, *Phys. Letters* **4** (1963).
- [46] Guy Deutscher, Andreev-Saint-James reflections: A probe of cuprate superconductors, *Rev. Mod. Phys* **77**, 109 (2005).
- [47] Morteza Salehi, Anisotropic angle-dependent Andreev reflection at the ferromagnet/superconductor junction on the surface of topological insulators, *Phys. Scr.* **98**, 025822 (2023).
- [48] M. Titov, A. Ossipov, and C. W. J. Beenakker, Excitation gap of a graphene channel with superconducting boundaries, *Phys. Rev. B* **75**, 045417 (2007).
- [49] Morteza Salehi, Planar Hall supercurrent and $\delta\phi$ -shift in the topological Josephson junction, *J. Magn. Magn. Mater.* **621**, 172915 (2025).
- [50] C. W. J. Beenakker, Specular Andreev Reflection in Graphene, *Phys. Rev. Lett.* **97**, 067007 (2006).
- [51] Moitri Maiti and K. Sengupta, Josephson effect in graphene superconductor/barrier/superconductor junctions: Oscillatory behavior of the Josephson current, *Phys. Rev. B* **76**, 054513 (2007).
- [52] R. A. Sepkhanov, Ya B. Bazaliy, and C. W. J. Beenakker, Extremal transmission at the Dirac point of a photonic band structure, *Phys. Rev. A* **75**, 063813 (2007).
- [53] M. Salehi and S. A. Jafari, Quantum transport through 3D Dirac materials, *Ann. Phys.* **359**, 64 (2015).
- [54] Jacob Linder, Takehito Yokoyama, Daniel Huertas-Hernando, and Asle Sudbø, Supercurrent Switch in Graphene pi Junctions, *Phys. Rev. Lett.* **100**, 187004 (2008).
- [55] Akira Furusaki and Masaru Tsukada, Dc Josephson effect and Andreev reflection, *Solid State Commun.* **78**, 299-302 (1991).
- [56] V. Prokić, A. I. Buzdin, and L. Dobrosavljević-Grujić, Theory of the pi junctions formed in atomic-scale superconductor/ferromagnet superlattices, *Phys. Rev. B* **59**, 587 (1999).